Journal of Pharmaceutical Sciences 109 (2020) 785-796

Contents lists available at ScienceDirect

Journal of Pharmaceutical Sciences

journal homepage: www.jpharmsci.org

Pharmaceutical Biotechnology

# An Experimental-Based Approach to Construct the Process Design Space of a Freeze-Drying Process: An Effective Tool to Design an Optimum and Robust Freeze-Drying Process for Pharmaceuticals

Getachew Assegehegn [1, *], Edmundo Brito-de la Fuente [1], José M. Franco [2], Críspulo Gallegos [1]

[1] Fresenius-Kabi Deutschland GmbH, Product and Process Engineering Center, Global Manufacturing Pharmaceuticals, Bad Homburg, Germany
[2] Departamento de Ingeniería Química, Pro2TecS-Chemical Product and Process Technology Research Centre, Complex Fluid Engineering Laboratory, Universidad de Huelva, Huelva, Spain

ARTICLE INFO

*Article history:*
Received 28 May 2019
Revised 2 July 2019
Accepted 2 July 2019
Available online 6 July 2019

*Keywords:*
freeze-drying
lyophilization
quality-by-design
formulation
processing
mathematical models(s)

ABSTRACT

The application of quality by design (QbD) is becoming an integral part of the formulation and process development for pharmaceutical products. An essential feature of the QbD philosophy is the design space. In this sense, a new approach to construct a process design space (PDS) for the primary drying section of a freeze-drying process is addressed in this paper. An effective customized design of experiments (DoE) is developed for freeze-drying experiments. The results obtained from the DoE are then used to construct the product-based PDS. The proposed product-based PDS construction approach has several advantages, including (1) eliminating assumptions on the heat transfer coefficient and dried product resistance, as it is constructed from experimental results specifically obtained from a given formulation, yielding more realistic and reliable results and (2) PDS construction based on a narrow range of product temperatures and considering the variations in product temperature and sublimation rate of vials across a shelf. This guarantees the effectiveness and robustness of the process and facilitates the process scale-up and transfer. The PDS developed herein was experimentally verified. The PDS predicted parameters were in excellent agreement with the experimentally obtained parameters.


## Introduction

Freeze-drying or lyophilization is a drying unit operation that is frequently used in pharmaceutical and biopharmaceutical industries to convert labile liquid formulations into a solid state with the aim of improving their long-term storage stability.[1,2] Despite being a method of high relevance for these industries, freeze-drying is an energy intensive, time consuming, and economically expensive process.[3,4] Therefore, the rational design and optimization of the freeze-drying process is of paramount importance. It is understandable that a sound knowledge of a formulation and its critical properties are essential for the efficient and rational design of a freeze-drying process.[5-9] Formulation critical properties include the freezing behavior of the formulation (phase separation, protein denaturation, and pH shift), glass transition temperature of the maximally freeze-concentrated solution ($T_g'$), collapse temperature of the amorphous formulation ($T_c$), eutectic temperature of the crystalline formulation ($T_{eu}$), stability of the active ingredients during preparation, and properties of the excipients. Knowledge of such formulation properties and the freeze-drying process itself significantly eases the design of a robust and optimum process. Whereas an optimum process minimizes the process time, a robust process addresses minor process deviations and maintains the predefined quality target product profiles (QTPP).

The primary drying step of the freeze-drying process is, typically, the most critical and longest processing step. Consequently, the majority of the optimization efforts are performed in this step. As reviewed in previous papers,[10,11] the freezing step has a significant effect on the primary drying rate; this is attributed to the morphology, and the number and size of ice crystals formed during the freezing step. The ice crystals leave a porous structure of dried product upon sublimation, which determines the permeability and resistance to water vapor flow through the dried product. The larger the ice crystals formed during the freezing, the larger the pore radius of the porous dried product and, hence, the lower the resistance to water vapor flow. This facilitates the drying rate during the sublimation step of the freeze-drying process. In general, the influence of the freezing step on the different freeze-

* *Correspondence to:* Getachew Assegehegn (Telephone: +4961726087381).
*E-mail address:* getachew.assegehegn@fresenius-kabi.com (G. Assegehegn).

https://doi.org/10.1016/j.xphs.2019.07.001
0022-3549/

**Nomenclature**

| | |
|---|---|
| CQAs | Critical quality attributes |
| DoE | Design of experiments |
| DS | Design space |
| $K_v$ | Vial heat transfer coefficient |
| MF1 | Model formulation 1 (10% (w/w) trehalose solution) |
| MF2 | Model formulation 2 (20% (w/w) sucrose solution) |
| $\dot{m}$ | Overall mass transfer rate (sublimation rate) from a vial |
| $P_c$ | Chamber pressure |
| PDS | Process design space |
| $P_i$ | Vapor pressure of ice |
| QbD | Quality by design |
| QTPP | Quality target product profiles |
| $r$ | Pore radius of a dried product |
| $R_p$ | Resistance to mass transfer of the dried product |
| $T_c$ | Collapse temperature of an amorphous formulation |
| $t_d$ | Drying time of primary drying |
| $T_{eu}$ | Eutectic temperature |
| $T_g$' | Glass transition temperature of the maximally freeze-concentrated solution |
| $T_p$ | Product temperature |
| $T_Pave$ | Average product temperature during primary drying |
| $T_pt$ | Target product temperature |
| $T_s$ | Shelf temperature |

drying parameters can be summarized as shown in Equation 1. A more detailed analysis of Equation 1 is given in reference.[11]

$$\left.\begin{array}{l} r = f(\textit{ice crystal size}) \\ R_p = f\left(\dfrac{1}{r}\right) \\ T_p = f\left(R_p,\ \dfrac{1}{r}\right) \\ P_i = f(T_p,\ R_p) \\ \dot{m} = f\left(\dfrac{1}{R_p},\ T_p\right) \end{array}\right| \textit{Provided } T_s \textit{ and } P_c \textit{ are held constant} \quad (1)$$

where, $r$(cm) is the pore radius of the dried product; $R_p$(mbar·s/g) is the resistance to mass transfer of the dried product; $T_p$(°C) is the product temperature, $P_i$(mbar) is the vapor pressure of ice; $T_s$(°C) is the shelf temperature; $P_c$(mbar) is the chamber pressure; and $\dot{m}(g/s)$ is the overall mass transfer rate from a vial.

During the primary drying step, the chamber pressure, $P_c$, is reduced to trigger the sublimation of the ice crystals and, simultaneously, the shelf temperature, $T_s$, is increased to provide energy to the sublimation process. The endothermic sublimation of ice and the exothermic heat input processes are occurring in "close equilibrium." Thus, the change in product temperature during the primary drying is insignificant, provided that the shelf temperature and chamber pressure are held constant. One major factor for a slight change in product temperature during the primary drying could be the increase in dried product resistance caused by an increase in dried layer thickness.

In a freeze-drying process, the product temperature is indirectly controlled through the manipulation of the shelf temperature and chamber pressure. In the majority of cases, the manipulation of the shelf temperature and chamber pressure is realized through a trial and error approach, which leads to unnecessary long experimental setups. Further, the resulting freeze-drying process is neither robust nor efficient. In an attempt to minimize the trial and error experiments, researchers have developed mathematical models for the determination of the optimum processing conditions based on the governing heat and mass transfer equations.[4,12-28] In these mathematical models, 2 input parameters, namely the overall vial heat transfer coefficient and the resistance to mass transfer of the dried product, are experimentally determined. The overall vial heat transfer coefficient is typically determined from a water sublimation test, whereas the resistance to mass transfer of the dried product is determined using the drug formulation. The determination of these parameters from a nondrug formulation and from a single experimental run could lead to a significant error during the optimization of the process.[22] The authors' experimental results show up to 18% difference in the overall vial heat transfer coefficient determined from water sublimation tests and from drug formulation sublimation tests (see Table 1). Further, determination of the dried product resistance from a single experimental run may not represent different processing conditions. Processing at a product temperature close to the $T_c$ could introduce a microcollapse on the dried structure, yielding a considerably reduced dried product resistance compared with the dried products without microcollapse.

Following the roll out of the International Conference on Harmonization (ICH) Q8(R2), the application of quality by design (QbD) has become an integral part of the formulation and process development for pharmaceutical products.[29] An essential feature of the QbD philosophy is the design space, which is defined, according to ICH Q8(R2), as a multidimensional combination and interaction of input variables and process parameters that have been demonstrated to provide the assurance of critical product quality.[30] Given the high interest of the pharmaceutical industries in implementing the QbD concept in their formulation and process development platforms, there exists a requirement for a systematic, scientific, and result-based design space construction strategy.

To address this point for a freeze-drying process, this study presents a new approach for the construction of a process design space (PDS) using a customized design of experiments (DoE). A PDS is a space enclosed by critical input process parameters of a given process, within which the output parameters and the critical quality attributes (CQAs) of the product remain within the desired limit. A PDS ensures both process efficiency and product quality,

**Table 1**
Differences in Overall Vial Heat Transfer Coefficients ($K_v$) of a Drug Formulation and Water for Injection

| $P_c$ (mbar) | $T_s$ (°C) | Overall Vial Heat Transfer Coefficient, $K_v$*$10^4$ (cal/s.cm$^2$.K) | | |
|---|---|---|---|---|
| | | Drug Formulation | Water for Injection | Difference (%) |
| 0.05 | −10.0 | 1.895 | 1.934 | 2.06 |
| | −17.0 | 1.952 | 1.871 | 4.15 |
| | −20.0 | 2.127 | 1.869 | 12.1 |
| 0.10 | −10.0 | 3.044 | 3.044 | 0.00 |
| | −15.0 | 2.847 | 3.093 | 8.64 |
| | −20.0 | 3.131 | 3.165 | 1.09 |
| | −24.0 | 2.764 | 3.182 | 15.1 |
| 0.15 | −15.0 | 4.169 | 4.624 | 10.9 |
| | −18.0 | 4.508 | 4.229 | 6.19 |
| | −25.0 | 3.485 | 4.144 | 18.9 |

Note that the experiments were performed using identical vials and stoppers. Authors' own experimental results. $P_c$ is chamber pressure and $T_s$ is shelf temperature.

and, hence, its advantages and applications during the freeze-drying of pharmaceutical products are significant. Because freeze-drying is an energy intensive process, designing the most optimum freeze-drying process is certainly one of the highest priorities for pharmaceutical industries. In this regard, a PDS provides an opportunity to define optimum process parameters while maintaining product quality. Further, a PDS significantly eases the freeze-drying process scale-up and transfer and ensures consistent product quality during large-scale commercial manufacturing. A PDS provides information on how possible process deviations during scale-up, transfer, or manufacturing influence the output parameters and CQAs and offers an opportunity for an early and systematic mitigation system for the case where the output parameters and CQAs are outside the PDS. Possible process deviations during scale-up, transfer, or manufacturing could be caused by differences in freezing conditions at lab and manufacturing scale and differences in equipment design. In such circumstances, equipment characterization is necessary to assess the differences between equipment and to adjust the processing conditions. Adjustment of the processing conditions could be significantly facilitated using the PDS.

In a freeze-drying process, it is important to consider that a PDS contains the input parameters that provide the maximum possible sublimation rate during the primary drying step. As can be deduced from Equation 1, the sublimation rate is dependent on several parameters, namely, ice vapor pressure or product temperature, chamber pressure, and dried product resistance to mass transfer. To maximize the sublimation rate during primary drying, it is important to execute at the highest vapor pressure of ice (this corresponds to the highest product temperature) and at the lowest chamber pressure. However, the maximum product temperature during primary drying is limited by the $T_c$ of the amorphous formulations or the $T_{eu}$ of the crystalline formulations. Conversely, the minimum chamber pressure is limited by the capability of the freeze-drying equipment.[31-33] In this sense, a PDS offers a method to identify the product and equipment limitations and to select the most optimized and robust process parameters for a given formulation.

Although profound prior scientific knowledge of both formulation and process is indispensable for building an effective DoE, it also significantly assists in minimizing the number of experiments necessary to construct a PDS. Using an effective DoE, less than 20 freeze-drying experiments can be performed to develop the PDS of a pharmaceutical formulation. As mentioned earlier, the primary drying is the most critical phase in terms of process economics and overall product quality. Thus, the focus of this study is on the construction of the PDS for the primary drying phase of the freeze-drying process. Although the mathematical models provide an opportunity to simulate several combinations of input process variables during the PDS construction, their success is highly dependent on the accuracy of the model input parameters and the assumptions of the model equations. In this sense, the experimental-based PDS construction approach detailed in this study offers an alternative method for the construction of a freeze drying PDS. In addition, although the mathematical models may need fewer experimental setups than the experimental approach presented herein, the advantages of the experimental approach over the mathematical models are several folds. These include (1) the utilization of unique and easy procedures to construct a PDS using the data obtained solely from freeze-drying experiments of a given drug product. This eliminates the assumptions on heat transfer coefficient and dried product resistance, thus providing highly accurate results. For this reason, the PDS developed in this study is termed a product-based PDS; (2) unlike the current representation of a freeze-drying PDS, this study uses shelf temperature versus chamber pressure curves with narrow ranges of product temperatures as contour lines. This facilitates the selection of the most effective and optimized process parameters for a given formulation; and (3) the PDS presented herein incorporates the variation in product temperatures and sublimation rates of vials at different locations of a shelf. This guarantees the robustness of the process and facilitates the process scale-up and transfer. Moreover, presenting a product-based PDS offers more realistic and reliable results if there is an intention of using the PDS for regulatory purposes.

Finally, it is worth pointing out that Chang and Fischer reported construction of a freeze-drying PDS based on experimental approach, aiming to explain the use of a single-step freeze drying cycle for a crystalline formulation (i.e., use of high shelf temperature [as high as 40°C] and low chamber pressure to avoid using secondary drying).[34] Consequently, it is apparent that the approach followed by Chang and Fischer is based on a rather different concept.

## Materials and Methods

### *Materials*

Sucrose was purchased from VWR (Darmstadt, Germany), and trehalose was purchased from Pfanstiehl, Inc. (Waukegan, IL). The 2 raw materials were used without further treatment. Water for injection was obtained from Fresenius Kabi Deutschland GmbH (Friedberg, Germany). All vials used in this study were 10-mL tubing vials purchased from SCHOTT AG (Mainz, Germany). The stoppers were Igloo single vented gray stoppers from West Pharmaceutical Services, Inc. (West Whiteland Township, PA).

Two model formulations were used for the development of the PDS. Model formulation 1 (MF1) was a 10% (w/w) trehalose solution; model formulation 2 (MF2) was a 20% (w/w) sucrose solution. Water for injection was used to prepare all the solutions used in this study. Aiming to remove particulate matters that could be introduced during preparation, the model formulations were filtered using 0.22 μm pore-size filters (PALL Corporation, Port Washington, NY) prior to filling the vials.

### *Methods*

#### *Differential Scanning Calorimetry*

The glass transition temperature of the frozen samples ($T_g$') was measured using a TA Instruments Q2000 series differential scanning calorimetry (DSC) with refrigerated cooling system (RCS) (TA Instruments, New Castle, DE). Sucrose and trehalose solutions were prepared as described previously, and a sample of 10-15 mg was weighed into aluminum sample pans, which were then hermetically sealed. An empty, hermetically sealed, pan was used as a reference. The RCS was set on continuous mode, and the nitrogen supply was set to 50 mL/min. The solution samples were first equilibrated at 40°C for 2 min and then frozen to −60°C at a rate of 20°C/min. The frozen samples were held at −60°C for 10 min before heating to 40°C at a rate of 10°C/min. The $T_g$' values were determined using Universal Analysis software and were reported as the midpoint of the glass transition curve.[35]

#### *Freeze-Drying Microscopy*

The collapse temperature ($T_c$) of the model formulations was determined using a Lyostat 2 freeze-drying microscopy (Biopharma Technology Ltd., Winchester, UK). Sucrose and trehalose solutions were prepared as described previously, and a sample of 2 μL was placed on a quartz cover slip and covered using a glass cover slip. To allow sublimation of the sample, a 70 μm thick metal spacer was placed between the quartz and glass cover slips. The solution samples were frozen to −40°C at a rate of 20°C/min and held for

5 min. After freezing, the vacuum was reduced to approximately 0.1 mbar and maintained at this condition until an approximately 2-3 mm dry layer thickness was achieved. The samples were further heated at 5°C/min to a temperature marginally less than the $T_g$' obtained from DSC, and then the heating rate was decreased to 0.5°C/min, aiming to observe a structural change at a higher temperature resolution. The samples were heated until complete structural damage was observed. Images of the samples were captured throughout the experiment, and the collapse temperature ($T_c$) was defined as the temperature where a clearly observable structural change of the frozen solution was observed.

*Freeze-Drying Experiment*

All freeze-drying experiments were performed using an HOF laboratory freeze dryer with a total usable shelf area of 0.36 $m^2$ (HOF Sonderanlagenbau GmbH, Lohra, Germany). The freeze dryer was equipped with a Pirani gauge for chamber pressure control and 3 type K thermocouples for the measurement of the product temperature. Freeze-drying experiments of both model formulations were performed using 10-mL tubing vials. For each of the model formulations, 176 vials (1 fully loaded shelf) were filled with 4 mL solution and placed on 1 of the 4 shelves of the freeze dryer. During the sublimation rate determination experiments, the fill volume was selected to be higher than the design fill volume (3 mL) to bring equivalence in dried product resistance and sublimation rate. For example, consider a sublimation experiment that was stopped after an average 60% of a given (5 mL) fill volume was sublimed. This is equivalent to a complete sublimation of 3 mL fill volume and, thus, brings equivalence in dried layer thickness (i.e., dried layer resistance) and sublimation rate. The freeze dryer had an acrylic chamber door, and to reduce the effect of radiation, the door was covered with a 4-mm thick polystyrene foam block and an aluminum foil. Eight wireless thermologgers (Lives International, Timis, Romania) and the 3 type K thermocouples were used to measure product temperatures. Although the presence of temperature probes could impact the freezing and drying behavior of the probed vials, such impact could be minimized by using thin temperature probes. Thus, both the type K thermocouples and wireless thermologgers used in this study were less than 1 mm thick. Product temperatures using the wireless thermologgers were measured every 20 s. The freezing step was held constant for all freeze-drying experiments as follows: 1°C/min down to −10°C and 90 min holding time; further freezing to −40°C at 1°C/min and 240 min holding time. Conversely, the primary drying was changed according to the DoE, as indicated in Table 2. The shelf surface temperatures (Fig. 4) were measured using the wireless thermologgers in a fully loaded shelf. For this purpose, the thermologgers were inserted into bottomless 10-mL vials, and they were arranged to have a clear contact with the shelf surface.

*Determination of Sublimation Rate*

The sublimation rate was determined gravimetrically. For this purpose, 50 selected sample vials were weighed before and after the freeze-drying experiments. The sample vials were systematically placed to represent different vial groups, which could have different sublimation rates and product temperatures, within the vial array. Figure 1 displays the placement of the sample vials and thermocoupled vials for all the experiments performed in this study. For example, in Figure 1, vials numbered 1-8 represent a vial group referred to as "*front edge*," vials 9-17 represent "*side edge outer*," vials 18-26 represent "*side edge inner*," vials 27-42 represent "*center*," and vials 43-50 represent "*rear edge*." Maximum, minimum, and average sublimation rates of each vial group were calculated from the sublimation rates obtained from the numbered vials of the same group (cf. Fig. 1). A laboratory analytical balance (Sartorius AG, Göttingen, Germany) was used to weigh the sample vials. The sublimation process was terminated by backfilling the product chamber using dry nitrogen, and the vials were heated to 20°C before the product chamber door was opened. This step was included to prevent condensation from the surrounding moisture from forming on the cold stoppers and penetrating into the extremely hygroscopic dried product. The freeze dryer available did not have an automatic stoppering mechanism. As a result, once the product chamber door was opened, the sample vials were taken out of the chamber, immediately fully stoppered and re-weighed.

**Table 2**
Custom Designed Full-Factorial Design of Experiments for Model Formulation 1 and Model Formulation 2

| Experiment Number | Primary Drying Input Parameters | | Primary Drying Output Parameters |
|---|---|---|---|
| | $P_c$ (mbar) | $T_s$ (°C) | |
| 1 | 0.05 | −5.0[a] | • Product temperature of front edge and center vials<br>• Sublimation rate of front edge and center vials |
| 2 | | −10.0 | |
| 3 | | −13.0[b] | |
| 4 | | −15.0 | |
| 5 | | −20.0 | |
| 6 | 0.08 | −10.0 | |
| 7 | | −15.0 | |
| 8 | | −20.0 | |
| 9 | | −25.0 | |
| 10 | 0.10 | −15.0 | |
| 11 | | −17.0 | |
| 12 | | −20.0 | |
| 13 | | −25.0 | |
| 14 | 0.15 | −17.0 | |
| 15 | | −20.0 | |
| 16 | | −25.0 | |
| 17 | | −30.0 | |
| 18 | 0.20 | −20.0 | |
| 19 | | −25.0 | |
| 20 | | −30.0 | |

$P_c$ is chamber pressure and $T_s$ is shelf temperature.
[a] Experiment only for model formulation 1.
[b] Experiment only for model formulation 2.

It is well-known that dried product resistance and product temperature increase when product dried layer thickness increases.[19,22,36] Therefore, to include the maximum effect of the dried product resistance during the determination of the sublimation rate, the sublimation experiments were stopped once the dried layer of the front edge vials was close to the vial bottom. This was performed by visually observing the dried layer of the front edge vials. At the end of the sublimation experiments, up to 70 wt% of the initial water content of the edge vials was removed, whereas, for center vials, up to 50 wt% of the initial water content was removed. Further, this procedure allows determination of consistent loss of water during the different sublimation experiments. The exact drying time for the calculation of the sublimation rate was obtained from the product temperature profile of the wireless thermologgers. Primary drying time, by definition, starts when the shelf temperature attains the desired shelf set point temperature for primary drying. Thus, regardless of the product temperature, the starting time for the calculation of the sublimation rates was defined as the time at which the shelf temperature attained the desired set point temperature. It was experimentally determined that at low chamber pressure and low shelf temperature, up to 4 h were required to achieve a pseudo steady-state condition in product temperature. Whereas, up to 2 h were required to attain a pseudo steady-state condition in product temperature at high chamber pressure and high shelf temperature conditions. Although the time required to achieve a pseudo steady state in product temperature was highly dependent on the processing conditions and formulation solid content, the values obtained in this study

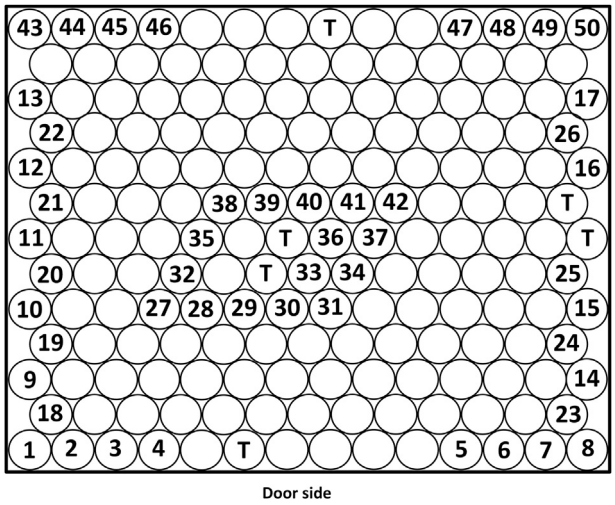


**Figure 1.** Vial placement for the sublimation experiments of this study. "Numbered vials" represent vials weighed before and after the freeze-drying experiment. "T-signed vials" represent vials with thermocouples for product temperature measurement of the different groups of vial arrays.

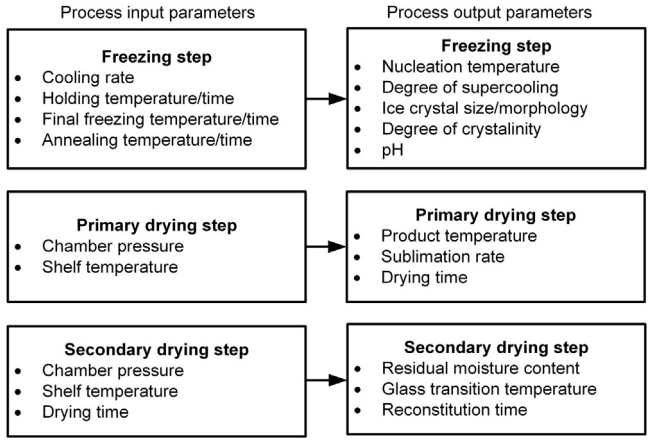


**Figure 2.** Critical input and output process parameters of a typical freeze-drying process.

were significantly longer than the values reported in the literature.[37] Therefore, such definition of the starting time considers the real effect of different processing conditions and formulations on the sublimation rate before the product temperature attained a pseudo steady-state condition. That is, the calculation of the sublimation rates considered the transition period at the beginning of the primary drying. Thus, any bias in sublimation rate calculation that could occur due to the transition period was avoided.

*Design of Experiments*

DoE is a structured analysis of experiments wherein input parameters are changed, and differences and variations in output parameters are measured. DoE allows the simultaneous determination of the effects of all potential input variables on the output responses, as well as investigations on how the process response changes as input variables fluctuate (random and systematic variation of the process parameters) within allowable limits. This requires a profound scientific background of the formulation and process, and, further, preliminary experiments using the specified drug formulation could be required to facilitate the development of an effective DoE. For a freeze-drying process, the critical process input and output parameters of the 3 steps are well known. They are depicted in Figure 2.

As the focus of this study was on the PDS development for the primary drying step, the DoE only considered the input and output parameters of the primary drying step of the freeze-drying process. Based on prior knowledge and preliminary experiments using the model formulations, a customized full-factorial DoE for both model formulations was developed as displayed in Table 2.

## Results and Discussion

*Characterization of Frozen Formulations*

Representative DSC thermograms for MF1 and MF2 are displayed in Figure 3i. For MF1, $T_g'$ was observed at a temperature of −29.2°C; for MF2, $T_g'$ was observed at a temperature of −32.4°C. The $T_g'$ values of MF1 and MF2 obtained in this study were in excellent agreement with previously reported values.[35,38]

Freeze-drying microscopy images of MF1 and MF2 are displayed in Figure 3ii. The $T_c$ of both model formulations obtained in this study were also in excellent agreement with the values reported in the literature.[39] Table 3 presents the results of $T_g'$, $T_c$, and the range of maximum product temperature during primary drying for the two model formulations.

*Construction of Process Design Space for MF1*

During the construction of the freeze-drying PDS, the limitations imposed by the freeze-dryer and formulation were considered. Patel and Pikal[40] reported that the majority of manufacturing dryers cannot control chamber pressures less than 0.06 mbar and that there is no additional advantage in sublimation rate for chamber pressures greater than 0.40 mbar. To verify these limitations, preliminary experiments were performed as follows: (1) a sublimation test using pure water at a chamber pressure of 0.05 mbar and a shelf temperature of −10°C. This test provided an average sublimation rate of 0.319 g/h·vial, which exceeds the expected average sublimation rate of the model formulations at the same chamber pressure. Therefore, it can be safely assumed that 0.05 mbar and greater chamber pressures would not experience chocking flow for the expected sublimation rates of the model formulations studied and (2) sublimation tests using both model formulations at a chamber pressure of 0.25 mbar and a shelf temperature of −25°C. Although these processing conditions yielded average product temperatures close to $T_c$ (−29.7°C for MF1 and −31.0°C for MF2), the corresponding average sublimation rates (0.074 g/h·vial for MF1 and 0.089 g/h·vial for MF2) were considerably less than the sublimation rates obtained at lower chamber pressures and similar product temperatures. Therefore, chamber pressures greater than 0.25 mbar would have no benefit from a sublimation rate point of view.

The DoE displayed in Table 2 was developed considering the information obtained from the previously mentioned preliminary experiments. Representative results of the freeze-drying experiments are presented in Table 4. The results for all the processing conditions displayed in the DoE (Table 2) were obtained in a similar manner (not indicated herein) and further processed.

The results displayed in Table 4 indicate remarkable differences in $T_p ave$ and the sublimation rates between the front edge and center vials. As supported by the experimental results displayed in Figure 4 and in the literature,[41-44] even in a freeze-drying process with a minimum effect of radiation, there could be significant spatial variation in the shelf surface temperature. Cold spots were observed at the center of the shelf, indicating a temperature of approximately 4°C colder than the hot spots, which were observed at the front edge

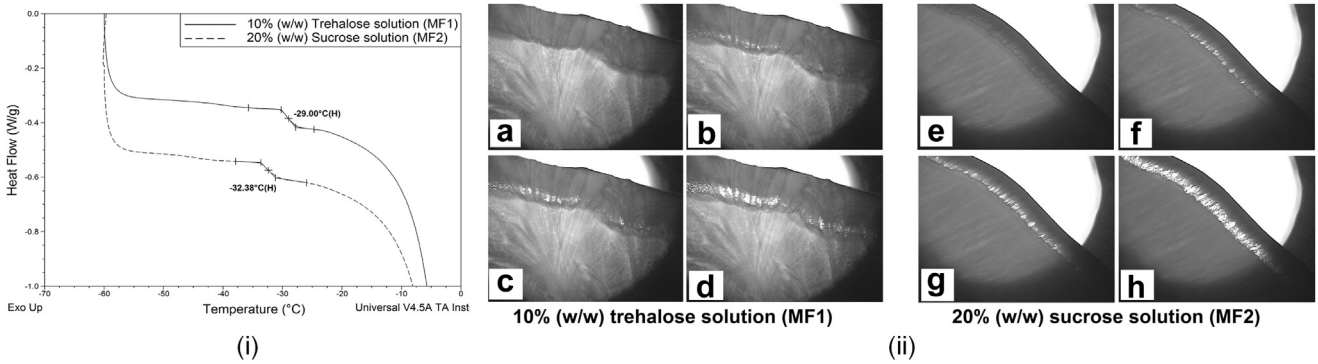


**Figure 3.** Characterization of frozen formulations. (i) DSC thermograms for MF1 (solid line) and for MF2 (dashed line). (ii) Freeze-drying microscopy images for MF1, (a) intact structure at T = −28.5°C, (b) onset of collapse at T = −28.0°C, (c) collapse at T = −27.5°C, and (d) significant damage at T = −27.0°C and for MF2, (e) intact structure at T = −31.8°C, (f) onset of collapse at T = −31.4°C, (g) collapse at T = −31.1°C, and (h) significant damage at T = −30.6°C.

of the shelf. These spatial shelf surface temperature variations could be attributed to the large thermal demand of the vials located at the center of the shelf compared with the vials located at the edge. The center vials have a higher vial packing density (number of vials per unit area). Hence, they absorb much larger energy during ice sublimation compared with edge vials. This, in turn, leads to different product temperatures and sublimation rates of the vials placed at different locations across a shelf (see Fig. 4).

Therefore, consideration of such variations during the construction of a PDS is critical in the design of a robust freeze-drying process. Further, as indicated in Table 4, the sublimation rate is dependent on the chamber pressure. Thus, depending on the chamber pressure, similar product temperatures can produce different sublimation rates. As displayed in Table 4 for MF1, a similar $T_p ave$ for front edge vials was obtained at Condition 1 ($T_s = -20°C/P_c = 0.10$ mbar) and Condition 2 ($T_s = -30°C/P_c = 0.20$ mbar). Analyzing Conditions 1 and 2, similar $T_p ave$ were obtained at different $T_s$ values. Thus, to yield similar $T_p ave$, a higher $P_c$ requires a lower $T_s$. This is because (1) when the chamber pressure increases, the heat transfer rate owing to gas conduction increases, leading to an increase in product temperature[45] and (2) at constant $P_i$, high chamber pressures reduce the driving force for mass transfer rate, $P_i(T_p) - P_c$. The reduction in the endothermic mass transfer rate decreases the energy consumption from a vial, leading to an increase in product temperature, unless $T_s$ is adjusted. It is important to note here that, although similar $T_p ave$ can be obtained at different $P_c$ values, the corresponding sublimation rate values can be significantly different. Referring to the aforementioned conditions, the sublimation rates of the front edge vials under Condition 1 are significantly greater than under Condition 2. Similarly, although the center vials at Condition 1 had reduced $T_p ave$, their sublimation rates were considerably greater compared with the center vials under Condition 2. This is attributed to the fact that at a given $T_p$, the driving force for mass transfer rate, $P_i(T_p) - P_c$, decreases as $P_c$ increases. Thus, for a given $T_p$, low $P_c$ and high $T_s$ produce a high mass transfer rate. Such knowledge and information for a specific drug product is essential to design the most optimized and robust freeze-drying process. A PDS can be used as a tool to choose the optimum process variables that yield the maximum possible mass transfer rate, without exceeding the maximum allowable product temperature during primary drying.

The construction of the PDS was started by plotting isotherms for the product temperature on a graph of shelf temperature versus chamber pressure, as displayed in Figure 5b. The product temperature isotherms were calculated from data obtained experimentally and represented the average product temperature of the front edge vials. The reason for selecting the front edge vials to define the product temperature was that this vial group had the highest product temperature in the vial arrays. Product temperatures were collected every 20 s. The average product temperature represents an average value of the product temperatures collected during the entire period of the sublimation test. Figure 5a presents the average product temperature of the front edge vials at the selected shelf temperature and chamber pressure. The results demonstrate an excellent linear relationship ($R^2 > 0.94$) of the average product temperature and shelf temperature at any given chamber pressure. Using regression analyses of the data points (solid lines, Fig. 5a), possible combinations of chamber pressure and shelf temperature that produce any desired product temperature can be calculated. This information was used to construct the graph of chamber pressure versus shelf temperature with the isotherms of the product temperatures (Fig. 5b).

As can be observed in Figure 5a, a change in the slope of the curves with increasing chamber pressure was observed. At relatively low chamber pressures, less than 0.08 mbar, the driving force for the sublimation rate is large, and thus the heat transfer becomes a rate-limiting factor of the drying process. In this case, as the excess sublimation process consumes additional input energy, large changes in shelf temperature are required to produce an observable change in product temperature. Conversely, although high chamber pressures enhance the heat transfer rate, which is attributed to improved heat transfer via gas conduction,[45] they significantly reduce the driving force for mass transfer. Thus, the mass transfer becomes a rate-limiting factor of the drying process, and any additional input energy, that is an increase in shelf temperature, has significant influence on the product temperature. This is evident from Figure 5a, where it can be observed that the curves at

**Table 3**
Values of $T_g'$, $T_c$, and the Range of Maximum Product Temperature During Primary Drying for MF1 and MF2

| Formulation | $T_g'$ (°C) | $T_c$ (°C) | Range of Maximum Product Temperature During Primary Drying (°C) |
|---|---|---|---|
| MF1 | −29.2 | −27.5 | −28.5 to −29.5 |
| MF2 | −32.4 | −31.1 | −31.5 to −32.5 |

$T_g'$ is the glass transition temperature of the maximally freeze-concentrated solution and $T_c$ is the collapse temperature.

**Table 4**
Results of Average Product Temperatures and Sublimation Rates at Selected Combinations of Chamber Pressure and Shelf Temperatures for MF1 and MF2

| $P_c$ (mbar) | $T_s$ (°C) | Formulation | Front Edge Vials | | | | Center Vials | | | |
|---|---|---|---|---|---|---|---|---|---|---|
| | | | $T_pave$[a] (°C) | Sublimation Rate (g/h·vial) | | | $T_pave$[a] (°C) | Sublimation Rate (g/h·vial) | | |
| | | | | Max[b] | Min[c] | Ave[d] | | Max[b] | Min[c] | Ave[d] |
| 0.10 | −15.0 | MF1 | −30.1 | 0.229 | 0.170 | 0.191 | −32.6 | 0.137 | 0.115 | 0.121 |
| | −17.0 | | −30.7 | 0.202 | 0.147 | 0.171 | −33.5 | 0.113 | 0.102 | 0.107 |
| | −20.0 | | −31.7 | 0.181 | 0.137 | 0.156 | −34.2 | 0.110 | 0.088 | 0.099 |
| | −25.0 | | −32.1 | 0.159 | 0.114 | 0.129 | −36.6 | 0.087 | 0.069 | 0.076 |
| 0.20 | −20.0 | | −28.9 | 0.223 | 0.175 | 0.193 | −29.9 | 0.134 | 0.120 | 0.125 |
| | −25.0 | | −29.8 | 0.165 | 0.125 | 0.138 | −31.4 | 0.085 | 0.081 | 0.078 |
| | −30.0 | | −31.7 | 0.094 | 0.069 | 0.078 | −33.5 | 0.046 | 0.026 | 0.042 |
| | −35.0 | | −34.7 | 0.055 | 0.035 | 0.044 | −36.6 | 0.018 | 0.015 | 0.016 |
| 0.10 | −15.0 | MF2 | −30.3 | 0.258 | 0.201 | 0.221 | −31.4 | 0.150 | 0.121 | 0.131 |
| | −17.0 | | −30.7 | 0.231 | 0.173 | 0.193 | −32.8 | 0.127 | 0.102 | 0.109 |
| | −20.0 | | −31.1 | 0.210 | 0.160 | 0.177 | −33.2 | 0.115 | 0.086 | 0.091 |
| | −25.0 | | −32.0 | 0.156 | 0.127 | 0.137 | −35.0 | 0.072 | 0.059 | 0.067 |
| 0.20 | −20.0 | | −30.1 | 0.272 | 0.208 | 0.232 | −30.8 | 0.153 | 0.138 | 0.144 |
| | −25.0 | | −31.3 | 0.174 | 0.145 | 0.157 | −32.3 | 0.105 | 0.081 | 0.092 |
| | −30.0 | | −32.2 | 0.131 | 0.095 | 0.108 | −33.8 | 0.052 | 0.041 | 0.045 |
| | −35.0 | | −34.5 | 0.077 | 0.046 | 0.057 | −36.7 | 0.018 | 0.014 | 0.016 |

$P_c$ is chamber pressure; $T_s$ is shelf temperature; $T_pave$ is the average product temperature.
[a] The average product temperatures ($T_pave$) for each vial group were calculated as the arithmetic average of the temperature measurements in the time range used for sublimation rate calculation.
[b] The maximum sublimation rates were the maximum value of the sublimation rates from each vial group.
[c] The minimum sublimation rates were the minimum value of the sublimation rates from each vial group.
[d] The average sublimation rates were calculated as the arithmetic average of the sublimation rates from each vial group.

low chamber pressure have larger slopes than the curves at high chamber pressures. This fact has a quantifiable effect from a process robustness point of view. That is, a freeze-drying process designed at relatively low chamber pressure is more robust to small shelf temperature variations than a freeze-drying process designed at relatively high chamber pressure.

The range of maximum product temperature during primary drying for MF1 was defined from −29.5°C to −28.5°C (see Table 3). Further, lower and higher chamber pressure limits were defined based on the equipment and process constraints. This information was used to impose formulation, process, and equipment constraints, and the PDS was defined as displayed in Figure 5b. From Figure 5b, the process parameters that yielded a low product temperature space and high product temperature space can be easily identified. In the former, the product temperature is less than the desired range and leads to an unnecessarily long primary drying time (inefficient process), whereas in the latter, the resulting high product temperature leads to product damage (collapse or meltback), which compromises product CQAs. Although it has been reported that collapse does not lead to a loss of CQAs for drug products,[40] additional experimental studies are required to study the effect of collapse on drug stability during storage.[46-53] Further, regulatory agencies require consistent, reproducible, and uniform cake appearance to ensure drug stability.[8]

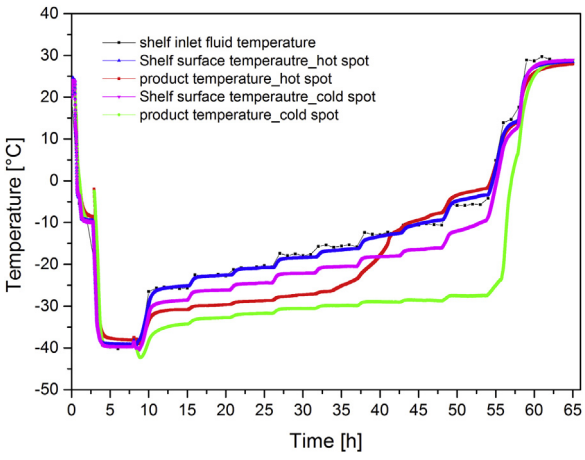


**Figure 4.** Experimental data showing significant spatial shelf surface temperature and product temperature differences across a shelf. Chamber pressure = 0.1 mbar.

From the PDS defined in Figure 5b, one would choose to use "high chamber pressure-low shelf temperature" or "low chamber pressure-high shelf temperature" combinations to achieve the same product temperature. However, depending on the chamber pressure, the same product temperature can produce different sublimation rates. At a given product temperature, low chamber pressure yields a high sublimation rate. Thus, a further definition of the PDS including values for sublimation rate is necessary. To include such information, the data of sublimation rates are plotted against experimental product temperatures, as displayed in Figure 6a. Figure 6a contains the average product temperature of the front edge vials in the *x*-axis and the minimum sublimation rate of the center vials in the *y*-axis. As reported in the literature[42-44,54] and determined experimentally in this study, the center vials have the lowest sublimation rate in the vial arrays. Therefore, Figure 6a allows consideration of the minimum sublimation rate during the construction of the PDS. This, in turn, avoids possible product damage owing to premature change to the secondary drying step. The choice of the average product temperature of the front edge vials in Figure 6a is because the product isotherms of the PDS (see Fig. 5b) are based on this parameter. Therefore, information on the sublimation rate of the center vials when the front edge vials achieve the target product temperature is required.

As indicated in Figure 6a, there is an excellent fitting of the experimental data ($R^2 > 0.95$) and regression analyses of the data were used to calculate the minimum sublimation rate of the center vials at a given chamber pressure and product temperature of the front edge vials. The initial PDS (Fig. 5b) was redefined after the sublimation rate values obtained from Figure 6a were included. The final PDS for MF1 is presented in Figure 6b.

The PDS defined in Figure 6b encompasses a wide range of $T_s$, $P_c$, and sublimation rate values. Thus, a control space within the PDS can be defined when the range of process parameters is small and well controlled. The control space is defined to encompass the

highest sublimation rates within the PDS. However, it is recommended that the consideration of edge process parameters to account for batch-to-batch process variations be avoided. Process parameters for the primary drying step can be defined within the control space as a set point. The set point can be selected anywhere within the control space. However, to consider intrabatch and interbatch variation in the process parameters, it is recommended to select the set point as the midpoint of the control space. At the set point, the minimum sublimation rate within the control space can be used to calculate the primary drying time.

*Construction of Process Design Space for MF2*

The experimental data obtained for MF2 were analyzed in a similar manner to the method followed for MF1. Accordingly, the PDS for the second formulation was obtained. It is presented in Figure 7.

*Experimental Verification of the PDSs for MF1 and MF2*

Because the calculations of the product temperatures and sublimation rates involve linear regression analyses, minor inaccuracies in the corresponding values could occur. Therefore, it is important to verify, experimentally, that the PDS obtained in this study yields the expected product temperatures and sublimation rates of the model formulations. Freeze-drying experimental runs were performed at selected set point values for both model formulations. The values of the set point parameters were selected from Figures 6b and 7, as follows:

- For MF1: $P_c = 0.075$ mbar, $T_s = 3$ °C, Fill volume = 3 mL
- For MF2: $P_c = 0.075$ mbar, $T_s = -16$ °C, Fill volume = 3 mL

The freezing protocol in these verification experiments was the same as the freeze protocol used for the construction of the PDS. This minimizes any possible variation of drying behavior owing to the freezing protocol. The product temperatures of the center and front edge vials were measured using wireless thermologgers (4 for each vial group). The sublimation rates of the center vials were determined gravimetrically and, for this purpose, 16 center vials were weighed before and after the experiment.

Figure 8 displays the product temperature profiles of MF1 and MF2 obtained from the verification experiments. Further, the estimated parameters from the PDS were compared with the parameters obtained from the verification experiments. They are presented in Table 5.

As indicated in Figure 8 and Table 5, there is an excellent agreement between the PDS-estimated and the experimentally determined values for both model formulations. This demonstrates that the procedures described in this article for the construction of an effective and product-based PDS, coupled with an effective DoE, produce highly accurate and reproducible results. This can enable process scientists to design freeze-drying processes for a given pharmaceutical drug formulation based on a scientific approach, using limited well-defined experimental runs.

*Utilization of the Lab PDS for Process Scale-Up and Transfer*

*Equipment Capability*

Mainly owing to their large capacity, chocking flow could be more pronounced at manufacturing scale freeze dryers. Therefore, it is critical to determine the capability of the target freeze dryer to control the $P_c$ at full load capacity and at typical freeze-drying sublimation rates. The determination of the capability of a target freeze dryer could be carried out using a one-point water sublimation test as follows: (1) fully load the target freeze dryer with pure water placed on a tray made from plastic; (2) freeze the water and allow complete solidification; (3) set the $P_c$ to 0 and increase the $T_s$ to +30°C or +40°C; and (4) observe the minimum $P_c$ and its stability, attained by the freeze dryer after the $T_s$ setpoint has been reached. Although the calculation of the exact value of the total vapor flow rate could be difficult, it could be assumed that the total vapor flow rate of pure water, at a $T_s$ value ranging from +30°C to +40°C and a controllable low $P_c$ is much higher than most of the typical vapor flow rates obtained using drug formulations. Thus, if a freeze dryer is able to attain and control a minimum $P_c$ of, for example, 50 µbar when pure water at a $T_s$ of +30°C or +40°C is used, it could be safely concluded that the occurrence of chocked flow for $P_c$ up to 50 µbar is highly unlikely when a drug formulation at typical primary drying $T_s$ values is used.

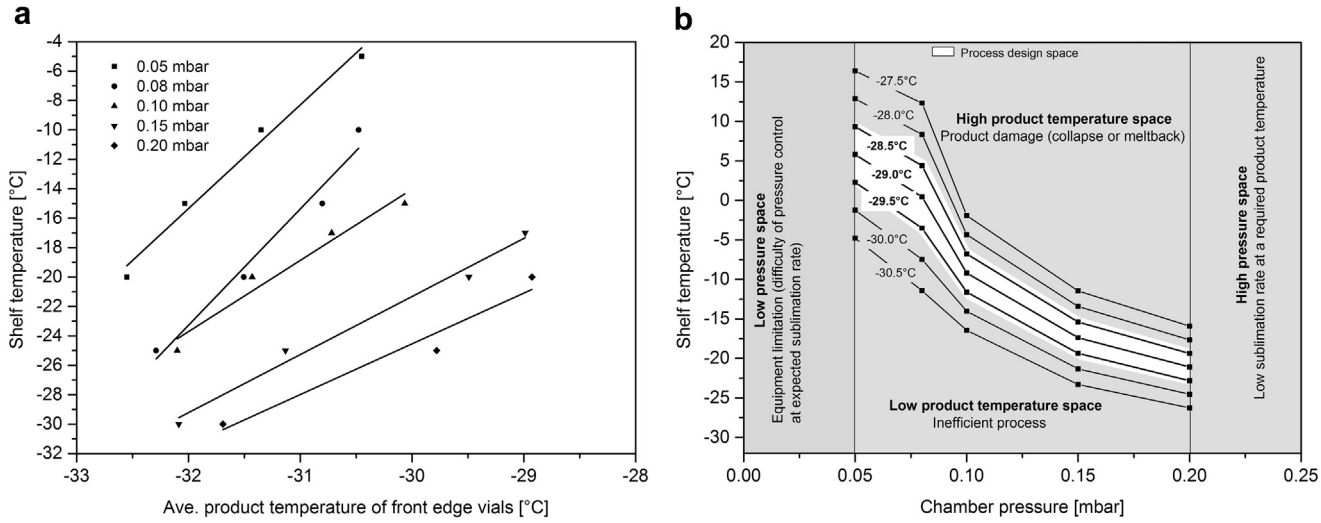


**Figure 5.** (a) Relationship between average product temperature of front edge vials and shelf temperature (at different chamber pressures) for MF1 and (b) PDS for primary drying of MF1 after formulation, process and equipment constraints.

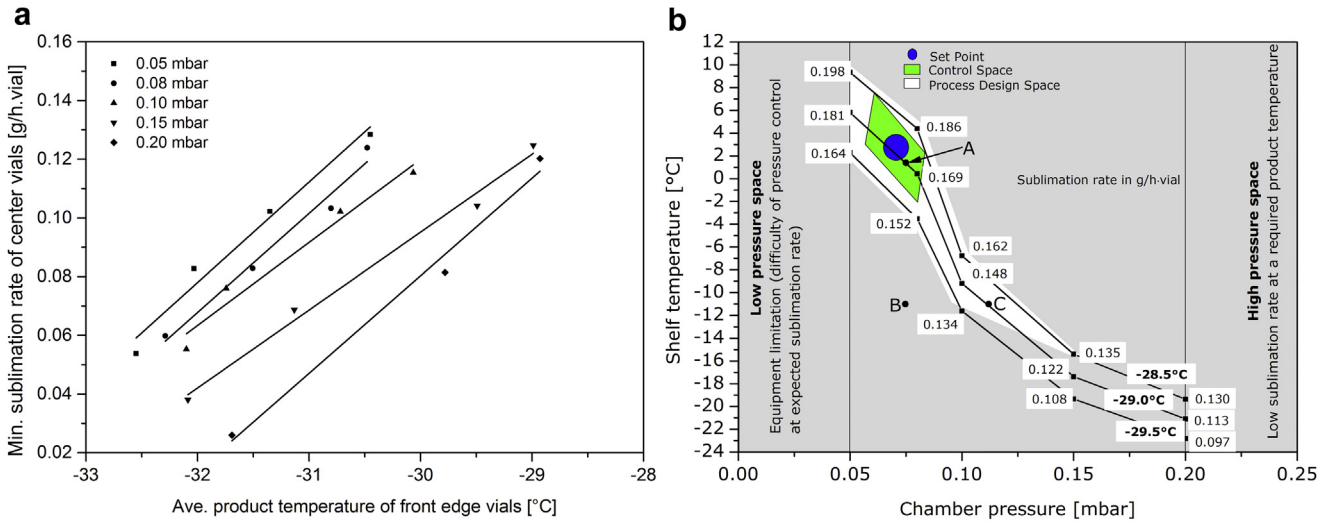


**Figure 6.** (a) Relationship of average product temperature of front edge vials and minimum sublimation rate of center vials (at different chamber pressures) for MF1. (b) Final process design space (PDS) for primary drying of MF1, taking into consideration minimum sublimation rate of center vials. Relatively minimum values of sublimation rate (mostly in the region of high chamber pressure) were removed from the originally defined PDS (Fig. 5b).

*Differences in Resistance to Mass Transfer of the Dried Product* ($R_p$) *and Overall Vial Heat Transfer Coefficient* ($K_v$)

The differences in $R_p$ and $K_v$ between laboratory and manufacturing scale freeze dryers are the major freeze-drying process scale-up and transfer factors. Differences in $R_p$ could be caused by variations in the degree of supercooling, which could be affected by differences in cleanness between laboratory and manufacturing environments. On the other hand, differences in $K_v$ could arise from differences in design and performance of the dryers. Differences in $R_p$ and $K_v$ during scale-up or transfer could be easily detected from $T_p$ response, provided that identical primary drying processing conditions (i.e., $T_s$ and $P_c$) are used. Thus, at the same processing conditions, an increase in $R_p$ is reflected by an increase in $T_p$. Because the vapor flow is more restricted at higher $R_p$, there is less energy consumption from the system, and most of the heat input is utilized to increase the $T_p$. Conversely, at low $R_p$, most of the heat input is consumed by the relatively higher sublimation rate (attributed to the lower resistance to vapor flow), and hence the $T_p$ becomes lower. An increase in $K_v$ at the same $T_s$ and $P_c$ leads to an increase in $T_p$ and vice versa. However, the influence of $K_v$ on freeze-drying process scale-up and transfer could be significantly minimized by using the same container-closure system and a laboratory scale freeze dryer with similar design and performance to a manufacturing scale freeze dryer. Therefore, the most important factor that could cause differences in $T_p$ during scale-up or transfer is $R_p$.

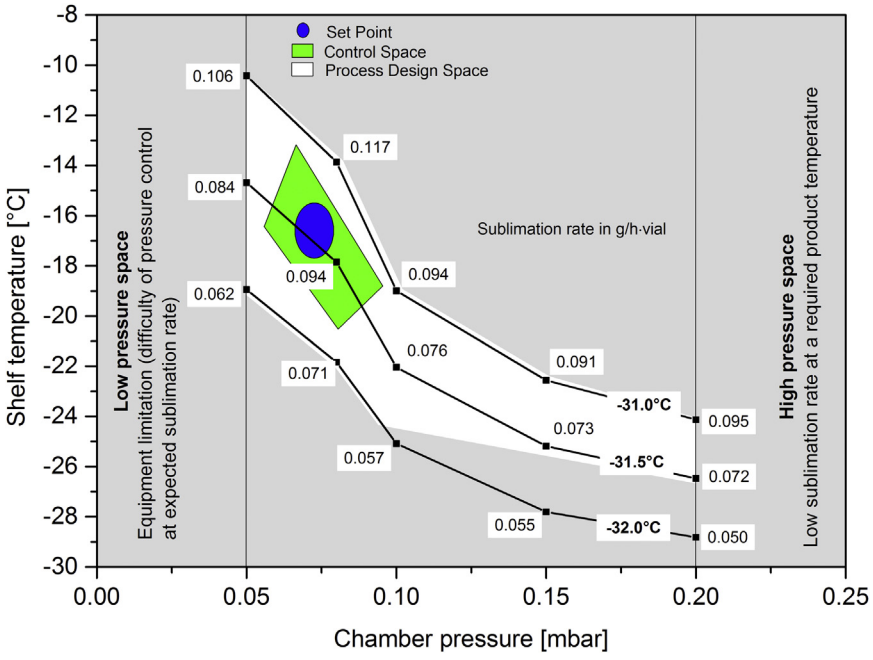


**Figure 7.** Final process design space (PDS) for primary drying of MF2, taking into consideration the minimum sublimation rate. Relatively minimum values of sublimation rate (mostly in the region of high chamber pressure) were removed from the originally defined PDS.

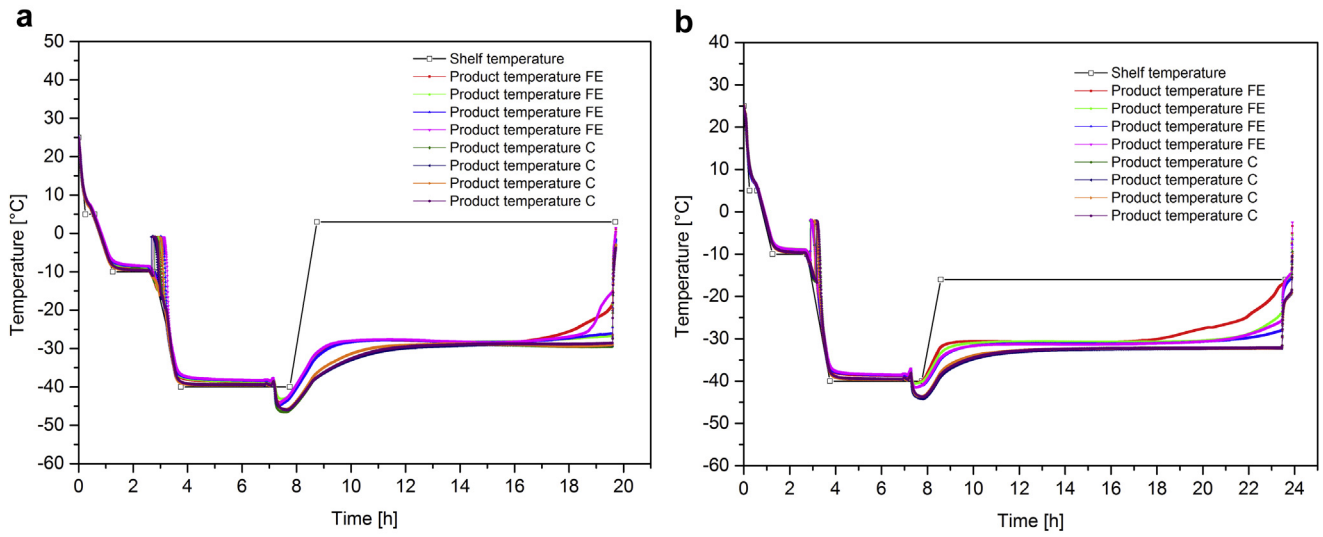


**Figure 8.** Experimental verification of the process design space (PDS). (a) Product temperature profiles of front edge vials (FE) and center vials (c) for MF1; (b) Product temperature profiles of front edge vials (FE) and center vials (c) for MF2.

From the above discussion, the $T_s$ (keeping $P_c$ constant) at the target freeze dryer that is needed to obtain the target product temperature ($T_pt$) could be different, and thus determination of the new $T_s$ and adjustment of the drying time ($t_d$) would be the major scale-up or transfer experiments. With this regard, the PDS developed at lab scale provides important information that could be utilized during the scale-up or transfer experiments: (1) the range of possible $T_s$ values that could be used to determine the new $T_s$; (2) the robustness of the formulation to $T_s$ changes; and (3) variation of sublimation rates at different processing conditions. Considering possible variations in $R_p$, a $T_s$ range from −12°C to +12°C at a $P_c$ = 0.075 mbar could yield the $T_pt$ for MF1 (cf. Fig. 6b). Such information could be utilized to perform a temperature ramp experiment using the target freeze drier to obtain the new $T_s$ value. Point A of Figure 6b shows that, at $P_c$ = 0.075 mbar, a $T_s$ around +1°C was required to yield a $T_p$ of −29.0°C. Assuming that the new $T_s$ value, at the target freeze dryer and $P_c$ = 0.075 mbar, required to yield a $T_p$ of −29.0°C was −11°C (Point B, Fig. 6b), the corresponding differences in sublimation rates and thus in $t_d$, of point A and point B could be adjusted using the PDS developed at lab scale. The reduction in sublimation rate caused by an increase in $R_p$ (thus a decrease in $T_s$) at constant $P_c$ (Point B, Fig. 6b) is equivalent to a reduction in sublimation rate caused by an increase in $P_c$ (thus a decrease in $T_s$) at constant $R_p$, provided that the $T_p$ is the same for both cases. Considering the same formulation, product temperature, and processing environment, the $R_p$ at laboratory scale can be assumed as fairly constant at the different processing conditions. Furthermore, assuming the reduction in $T_s$ at the target freeze dryer is due entirely to the increase in $R_p$, the sublimation rate at the new $T_s$ value (i.e., −11°C) and $T_p$ = −29.0°C from the PDS (point C, Fig. 6b) could be used to adjust the sublimation rate and the $t_d$ at the target freeze dryer.

## Conclusions

A new step-by-step procedure for the construction of a product-based PDS for the primary drying step was described. An effective DoE was developed, which could then be used to experimentally determine the necessary information for the construction of the PDS. The development of an effective DoE requires a profound scientific understanding of the formulation and process and perhaps requires only limited preliminary experiments. The proposed product-based PDS considers variations in product temperatures and sublimation rates within the vial arrays. With this regard, the product temperature of the front edge vials and sublimation rate of the center vials were used. This assures the effectiveness and the robustness of the PDS. Compared with the mathematical models that could require several freeze-drying experiments for optimization and verification, the product-based PDS detailed herein produced highly accurate results, demonstrating the potential for significant development time and material savings. Further, the PDS of a drug formulation based on experimental results presents more realistic and reliable data if there is an intention of using the PDS for regulatory agencies. Experimental

**Table 5**
Comparison of PDS-Estimated and Experimentally Determined Parameters at Set Point

| Formulation | PDS Estimated Values | | | | Experimentally Determined Values | | | | Differences (%) | | | |
|---|---|---|---|---|---|---|---|---|---|---|---|---|
| | FE | C | | | FE | C | | | FE | C | | |
| | $T_pave$ (°C) | $T_pave$ (°C) | $\dot{m}$(g/h·vial) | $t_d$[c] (h) | $T_pave$[a] (°C) | $T_pave$[a] (°C) | $\dot{m}$[b] (g/h·vial) | $t_d$[d] (h) | $T_pave$ | $T_pave$ | $\dot{m}$ | $t_d$ |
| MF1 | −28.7 | −31.0 | 0.169 | 16.0 | −28.4 | −30.1 | 0.177 | 15.3 | 1.05 | 2.90 | 4.73 | 4.38 |
| MF2 | −31.2 | −33.4 | 0.094 | 25.5 | −31.3 | −32.8 | 0.104 | 23.1 | 0.32 | 1.80 | 10.64 | 9.41 |

$T_pave$ is average product temperature; $\dot{m}$ is sublimation rate; $t_d$ is drying time of primary drying; FE is front edge vials; and C is center vials.
[a] $T_pave$ was obtained by averaging product temperatures obtained from 4 thermologgers.
[b] $\dot{m}$ is the minimum value of 16 sublimation rate values.
[c] $t_d$ is calculated based on the minimum sublimation rate within the control space and based on 3 mL fill volume.
[d] $t_d$ is calculated based on the minimum sublimation rate of the 16 experimentally determined sublimation rate values and based on 3 mL fill volume.

verifications of the PDS for the 2 formulations studied in this research were performed, and an excellent agreement between the PDS predicted values and experimentally determined values were achieved. Finally, coupled with an effective DoE, the proposed procedure for the construction of a product-based PDS considerably reduces development time and material requirements and significantly improves the accuracy, effectiveness, and robustness of the resulting freeze-drying process. Thus, process scale-up problems are minimized with the development of a PDS. Further, the resulting optimum and robust freeze-drying process has significant advantages in process cost and energy savings and in maintaining product quality consistency during a large-scale manufacturing process.

## Acknowledgment

Each of the authors confirms that there was no financial aid from an organization or technical assistance outside the authors themselves.

## References

1. Pikal MJ. Freeze-drying of proteins. Part I: process design. *BioPharm*. 1990;3:18-27.
2. Pikal MJ. Freeze-drying of proteins. Part II: formulation selection. *BioPharm*. 1990b;10:26-30.
3. Patel SM, Jameel F, Pikal MJ. The effect of dryer load on freeze drying process design. *J Pharm Sci*. 2010;99:4363-4379.
4. Mortier STFC, Van Bockstal PJ, Corver J, Nopens I, Gernaey KV, De Beer T. Uncertainty analysis as essential step in the establishment of the dynamic design space of primary drying during freeze-drying. *Eur J Pharm Biopharm*. 2016;103:71-83.
5. Tang X, Pikal MJ. Design of freeze-drying processes for pharmaceuticals: practical advice. *Pharm Res*. 2004;21:191-200.
6. Liu J. Physical characterization of pharmaceutical formulations in frozen and freeze-dried solid states: techniques and applications in freeze-drying development. *Pharm Dev Technol*. 2006;11:3-28.
7. Wang DQ. Formulation characterization. In: Rey L, May JC, eds. *Freeze Drying/Lyophilization of Pharmaceutical and Biological Products*. 3rd ed. London, UK: Informa Healthcare; 2010:233-253.
8. Goldman JM, More HT, Yee O, et al. Optimization of primary drying in lyophilization during early-phase drug development using a definitive screening design with formulation and process factors. *J Pharm Sci*. 2018;107:2592-2600.
9. Ward KR, Matejtschuk P. Characterization of formulations for freeze-drying. In: Ward K, Matejtschuk P, eds. *Lyophilization of Pharmaceuticals and Biologicals. Methods in Pharmacology and Toxicology*. New York: Humana Press; 2019:1-32.
10. Goshima H, Do G, Nakagawa K. Impact of ice morphology on design space of pharmaceutical freeze-drying. *J Pharm Sci*. 2016;105:1920-1933.
11. Assegehegn G, Brito-de la Fuente E, Franco JM, Gallegos C. The importance of understanding the freezing step and its impact on freeze drying process performance. *J Pharm Sci*. 2019;108:1378-1395.
12. Pikal MJ, Cardon S, Bhugra C, et al. The non-steady state modeling of freeze-drying: in-process product temperature and moisture content mapping and pharmaceutical product quality applications. *Pharm Dev Technol*. 2005;10:17-32.
13. Gieseler H, Kramer T, Pikal MJ. Use of Manometric Temperature Measurement (MTM) and SMART$^{TM}$ freeze dryer technology for development of an optimized freeze-drying cycle. *J Pharm Sci*. 2007;96:3402-3418.
14. Velardi SA, Barresi AA. Development of simplified models for the freeze-drying process and investigation of the optimal operating conditions. *Chem Eng Res Des*. 2008;86:9-22.
15. Kuu WY, Nail SL. Rapid freeze-drying cycle optimization using computer programs developed based on heat and mass transfer models and facilitated by Tunable Diode Laser Absorption Spectroscopy (TDLAS). *J Pharm Sci*. 2009;98:3469-3482.
16. Sundaram J, Shay YHM, Hsu CC, Sane SU. Design space development for lyophilization using DOE and process modeling. *Biopharm Int*. 2010;23:26-36.
17. Giordano A, Barresi AA, Fissore D. On the use of mathematical models to build the design space for the primary drying phase of a pharmaceutical lyophilization process. *J Pharm Sci*. 2011;100:311-324.
18. Koganti VR, Shalaev EY, Berry MR, et al. Investigation of design space for freeze-drying: use of modeling for primary drying segment of a freeze-drying cycle. *AAPS PharmSciTech*. 2011;12:854-861.
19. Fissore D, Pisano R, Barresi AA. Advanced approach to build the design space for the primary drying of a pharmaceutical freeze-drying process. *J Pharm Sci*. 2011;100:4922-4933.
20. Bosca S, Barresi AA, Fissore D. Fast freeze-drying cycle design and optimization using a PAT based on the measurement of product temperature. *Eur J Pharm Biopharm*. 2013;85:253-262.
21. Kodama T, Sawada H, Hosomi H, et al. Determination for dry layer resistance of sucrose under various primary drying conditions using a novel simulation program for designing pharmaceutical lyophilization cycle. *Int J Pharm*. 2013;452:180-187.
22. Kodama T, Sawada H, Hosomi H, et al. Optimization of primary drying condition for pharmaceutical lyophilization using a novel simulation program with a predictive model for dry layer resistance. *Chem Pharm Bull*. 2014;62:153-159.
23. Fissore D, Pisano R. Computer-aided framework for the design of freeze-drying cycles: optimization of the operating conditions of the primary drying stage. *Processes*. 2015;3:406-421.
24. Chen X, Sadineni V, Maity M, Quan Y, Enterline M, Mantri RV. Finite element method (FEM) modeling of freeze-drying: monitoring pharmaceutical product robustness during lyophilization. *AAPS PharmSciTech*. 2015;16:1317-1326.
25. Van Bockstal PJ, Mortier STFC, Corver J, Nopens I, Gernaey KV, De Beer T. Quantitative risk assessment via uncertainty analysis in combination with error propagation for the determination of the dynamic design space of the primary drying step during freeze-drying. *Eur J Pharm Biopharm*. 2017;121:32-41.
26. Arsiccio A, Pisano R. Application of the quality by design approach to the freezing step of freeze-drying: building the design space. *J Pharm Sci*. 2018;107:1586-1596.
27. Zhu T, Moussa EM, Witting M, et al. Predictive models of lyophilization process for development, scale-up/tech transfer and manufacturing. *Eur J Pharm Biopharm*. 2018;128:363-378.
28. Sharma P, Kessler WJ, Bogner R, Thakur M, Pikal MJ. Applications of the tunable diode laser absorption spectroscopy: in-process estimation of primary drying heterogeneity and product temperature during lyophilization. *J Pharm Sci*. 2019;108:416-430.
29. Patel S, Jameel F, Sane S, Kamat M. Lyophilization process design and development using QbD principles. In: Jameel F, Hershenson S, Khan M, Martin-Moe S, eds. *Quality by Design for Biopharmaceutical Drug Product Development. AAPS Advances in the Pharmaceutical Sciences Series*. 18. New York: Springer; 2015:303-329.
30. US Department of Health and Human Services, Food and Drug, Administration. Center for drug evaluation and research(CDER), center for biologics evaluation and research (CBER). In: *ICH Q8(R2) Pharmaceutical Development*. Silver Spring, MD: Food and Drug Administration (FDA); 2009.
31. Ganguly A, Alexeenko AA, Schultz SG, Kim SG. Freeze-drying simulation framework coupling product attributes and equipment capability: toward accelerating process by equipment modifications. *Eur J Pharm Biopharm*. 2013;85:223-235.
32. Ganguly A, Varma N, Sane P, Bogner R, Pikal M, Alexeenko A. Spatial variation of pressure in the lyophilization product chamber part 1: computational modeling. *AAPS PharmSciTech*. 2017;18:577-585.
33. Kshirsagar V, Tchessalov S, Kanka F, Hiebert D, Alexeenko A. Determining maximum sublimation rate for a production lyophilizer: computational modeling and comparison with ice slab tests. *J Pharm Sci*. 2019;108:382-390.
34. Chang BS, Fischer NL. Development of an efficient single-step freeze-drying cycle for protein formulations. *Pharm Res*. 1995;12:831-837.
35. Her LM, Nail SL. Measurement of glass transition temperatures of freeze-concentrated solutes by differential scanning calorimetry. *Pharm Res*. 1994;11:54-59.
36. Scutellà B, Trelea IC, Bourlès E, Fonseca F, Passot S. Determination of the dried product resistance variability and its influence on the product temperature in pharmaceutical freeze-drying. *Eur J Pharm Biopharm*. 2018;128:379-388.
37. Pikal MJ. Use of laboratory data in freeze-drying process design: heat and mass transfer coefficients and the computer simulation of freeze-drying. *J Parenter Sci Technol*. 1985;39:115-139.
38. Chang BS, Randall CS. Use of sub-ambient thermal analysis to optimize protein lyophilization. *Cryobiology*. 1992;29:632-656.
39. Adams GDJ, Ramsay JR. Optimizing the lyophilization cycle and the consequences of collapse on the pharmaceutical acceptability of Erwinia l-Asparaginase. *J Pharm Sci*. 1996;85:1301-1305.
40. Patel SM, Pikal MJ. Lyophilization process design space. *J Pharm Sci*. 2013;102:3883-3887.
41. Pikal MJ, Bogner R, Mudhivarthi V, Sharma P, Sane P. Freeze-drying process development and scale-up: scale-up of edge vial versus center vial heat transfer coefficients, Kv. *J Pharm Sci*. 2016;105:3333-3343.
42. Scutellà B, Plana-Fattoric A, Passota S, et al. 3D mathematical modelling to understand atypical heat transfer observed in vial freeze-drying. *Appl Therm Eng*. 2017;126:226-236.
43. Scutellà B, Passot S, Bourlés E, Fonseca F, Tréléa IC. How vial geometry variability influences heat transfer and product temperature during freeze-drying. How vial geometry variability influences heat transfer and product temperature during freeze-drying. *J Pharm Sci*. 2017;106:770-778.
44. Scutellà B, Bourlès E, Plana-Fattori A, et al. Effect of freeze dryer design on heat transfer variability investigated using a 3D mathematical model. *J Pharm Sci*. 2018b;107:2098-2106.
45. Pikal MJ, Roy ML, Shah S. Mass and heat transfer in vial freeze-drying of pharmaceuticals: role of the vial. *J Pharm Sci*. 1984;73:1224-1237.
46. Wang DQ, Hey JM, Nail SL. Effect of collapse on the stability of freeze-dried recombinant factor VIII and a-amylase. *J Pharm Sci*. 2004;93:1253-1263.
47. Schersch K, Betz O, Garidel P, Muehlau S, Bassarab S, Winter G. Systematic investigation of the effect of lyophilizate collapse on pharmaceutically relevant proteins I: stability after freeze-drying. *J Pharm Sci*. 2010;99:2256-2278.

48. Schersch K, Betz O, Garidel P, Muehlau S, Bassarab S, Winter G. Systematic investigation of the effect of lyophilizate collapse on pharmaceutically relevant proteins, part 2: stability during storage at elevated temperatures. *J Pharm Sci*. 2012;101:2288-2306.
49. Schersch K, Betz O, Garidel P, Muehlau S, Bassarab S, Winter G. Systematic investigation of the effect of lyophilizate collapse on pharmaceutically relevant proteins III: collapse during storage at elevated temperatures. *Eur J Pharm Biopharm*. 2013;85:240-252.
50. Ullrich S, Seyferth S, Lee G. Measurement of shrinkage and cracking in lyophilized amorphous cakes. Part I: final-product assessment. *J Pharm Sci*. 2015;104:155-164.
51. Patel SM, Nail SL, Pikal MJ, et al. Lyophilized drug product cake appearance what is acceptable? *J Pharm Sci*. 2017;106:1706-1721.
52. Duralliu A, Matejtschuk P, Williams DR. Humidity induced collapse in freeze dried cakes: a direct visualization study using DVS. *Eur J Pharm Biopharm*. 2018;127:29-36.
53. Haeuser C, Goldbach P, Huwyler J, Friess W, Allmendinger A. Imaging techniques to characterize cake appearance of freeze-dried products. *J Pharm Sci*. 2018;107:2810-2822.
54. Pikal MJ, Pande P, Bogner R, Sane P, Mudhivarthi V, Sharma P. Impact of natural variations in freeze-drying parameters on product temperature history: application of quasi steady-state heat and mass transfer and simple statistics. *AAPS PharmSciTech*. 2018;19:2828-2842.